NASA TECHNICAL NOTE

NASA TN D-8396

VELOCITY AND TEMPERATURE DISTRIBUTIONS OF COAL-SLAG LAYERS ON MAGNETOHYDRODYNAMIC GENERATOR WALLS

Carlson C. P. Pian and J. Marlin Smith

Lewis Research Center
Cleveland, Ohio 44135

NATIONAL AERONAUTICS AND SPACE ADMINISTRATION • WASHINGTON, D. C. • JANUARY 1977

1. Report No. NASA TN D-8396	2. Government Accession No.	3. Recipient's Catalog No.
4. Title and Subtitle VELOCITY AND TEMPERATURE DISTRIBUTIONS OF COAL-SLAG LAYERS ON MAGNETOHYDRODYNAMIC GENERATOR WALLS		5. Report Date January 1977
		6. Performing Organization Code
7. Author(s) Carlson C. P. Pian and J. Marlin Smith		8. Performing Organization Report No. E-8929
		10. Work Unit No. 506-25
9. Performing Organization Name and Address Lewis Research Center National Aeronautics and Space Administration Cleveland, Ohio 44135		11. Contract or Grant No.
		13. Type of Report and Period Covered Technical Note
12. Sponsoring Agency Name and Address National Aeronautics and Space Administration Washington, D.C. 20546		14. Sponsoring Agency Code

15. Supplementary Notes

16. Abstract

Approximate analytical expressions are derived for the velocity and temperature distributions in steady-state coal slag deposits flowing over MHD generator walls. Effects of slag condensation and Joule heating are included in the analysis. The transport conditions and the slag temperature at the slag-gas interface are taken to be known parameters in the formulation. They are assumed to have been predetermined either experimentally or from the slag properties and the gas dynamic calculations of the free-stream flow. The analysis assumes a power-law velocity profile for the slag and accounts for the coupling between the energy and momentum conservation equations. Comparisons are made with the more exact numerical solutions to verify the accuracy of the results.

17. Key Words (Suggested by Author(s)) Magnetohydrodynamic generators; Coal slag deposits; Velocity distributions; Temperature profiles; Electrical resistivity; Approximate analytical expression	18. Distribution Statement Unclassified - unlimited STAR Category 44		
19. Security Classif. (of this report) Unclassified	20. Security Classif. (of this page) Unclassified	21. No. of Pages 19	22. Price* $3.50

VELOCITY AND TEMPERATURE DISTRIBUTIONS OF COAL-SLAG LAYERS

ON MAGNETOHYDRODYNAMIC GENERATOR WALLS

by Carlson C. P. Pian and J. Marlin Smith

Lewis Research Center

SUMMARY

Approximate analytical expressions are derived for the velocity and temperature distributions in steady-state coal slag deposits flowing over magnetohydrodynamic generator walls. Effects of slag condensation and Joule heating are included in the analysis. The transport conditions and the slag temperature at the slag-gas interface are taken to be known parameters in the formulation. They are assumed to have been predetermined either experimentally or from the slag properties and the gas dynamic calculations of the free-stream flow. The analysis assumes a power-law velocity profile for the slag and accounts for the coupling between the energy and momentum conservation equations. Comparisons are made with the more exact numerical solutions to verify the accuracy of the results.

INTRODUCTION

The behavior of slag layers in magnetohydrodynamic (MHD) generator ducts has recently gained increased attention after the University of Tennessee Space Institutes' experiments showed the possibility of power generation from MHD generators coated with coal slag (ref. 1). Problems involved with analyzing these slag deposits are not straightforward because of the vast variation in physical properties and experimental conditions. Theoretical analysis, even with idealized assumptions, is complicated by the coupling of the slag momentum and energy equations through the strong dependence of the slag viscosity on the temperature. Hence, most investigators have relied on numerical procedures (refs. 2 and 3). Although analytical solutions provide more physical perceptivity, exact solutions for the velocity and temperature distributions within a slag layer have been obtained previously only by excluding slag condensation and Joule heating effects (ref. 4).

In the present report, approximate analytical expressions are derived for the veloc-

ity and temperature variations in steady-state slag layers. Effects of mass condensation and Joule heating are included in the analysis. The transport conditions and the slag temperature at the slag-gas interface are taken to be known parameters in the formulation. They are either experimentally measurable or determinable from the slag properties and the gas dynamic calculations of the free-stream flow. The analysis, based on the model of reference 5, assumes a power-law slag velocity profile and accounts for the coupling between the energy and momentum conservation equations. Comparisons are also made with the more exact numerical solutions of reference 4 to verify the accuracy of the present analysis.

GOVERNING EQUATIONS

Consider the steady slag flow over a smooth horizontal surface of infinite extent in the streamwise x-direction, as shown in figure 1. The assumption is made that the slag surface is acted upon by gas dynamic heating and shear stress at the slag surface τ_i from the concurrent gas flow. In addition, there may be mass transfer to the slag layer, at a rate m_i, from condensation of slag particles. The wall at $y = 0$ is maintained at temperature T_w. The value of T_w is dictated by the design of the wall segment and its coolant passages. The slag surface at $y = \delta$ is at temperature T_i and moves with velocity u_i. The value of T_i or δ is defined by the surface viscosity and the slag properties (ref. 6) or is experimentally measurable (ref. 7). The interfacial shear and the amount of mass transport to the slag layer are determinable from a Reynolds analogy treatment for a flat plate (refs. 2 and 6). From the same flat-plate, turbulent-boundary-layer analysis, the heat flux q is given by $H(T_\infty - T_i)$. Typical values of pertinent slag properties including the heat transfer coefficient H are presented in table I. Hence, we consider T_∞, τ_i, T_i, or δ, m_i, and T_w as given parameters in this formulation.

The once-integrated slag layer momentum equation, neglecting inertia forces at low Reynolds number, is

$$\mu \frac{\partial u}{\partial y} = \frac{\partial P}{\partial x} (y - \delta) + \tau_i + j_y B(y - \delta) \tag{1}$$

Taking $j_y \leq 1 \times 10^4$ A/m^2 and the characteristic values given in table I, the terms in equation (1) are found to be of the following magnitudes:

2

$$\frac{\partial P}{\partial x} (y - \delta) \sim P_a \times 10^{-4} \text{ pascals}$$

$$\tau_i \sim P_a \times 10^{-3} \text{ pascals}$$

$$j_y B(y - \delta) \sim 40 \text{ pascals}$$

where P_a is the gas pressure and varies from about 4×10^5 pascals at the generator entrance to 0.5×10^5 pascals at the exit (ref. 6). Thus, in a typical base-loaded MHD generator away from the duct exit the inertial forces, the pressure gradient dP/dx, and the $j \times B$ body force within the slag layer are all much smaller in magnitude than the shear force $\partial/\partial y(\mu\, \partial u/\partial y)$ and can be neglected in the momentum balance. Thermal gradients parallel to the surface are assumed to be much smaller than the normal gradients and are neglected in the energy equation. The governing equations of continuity, momentum, and energy, respectively, reduce to

$$\frac{\partial u}{\partial x} + \frac{\partial v}{\partial y} = 0 \tag{2}$$

$$\frac{\partial u}{\partial y} = \frac{\tau_i}{\mu(T)} \tag{3}$$

and

$$k \frac{\partial^2 T}{\partial y^2} = \rho c v \frac{\partial T}{\partial y} - \frac{j^2}{\sigma} \tag{4}$$

where the thermal conductivity k is taken to be independent of temperature and composition. The viscosity coefficient μ, being a strong function of temperature, is written as

$$\mu = \mu_i \left(\frac{T_i}{T}\right)^\beta \tag{5}$$

where the exponent β has a value between 17 and 20 for typical slags in the temperature range under study (ref. 6). The mass balance of the slag layer is given by

$$\frac{\partial}{\partial x} \int_0^{\delta} u \, dy = \frac{m_i}{\rho} \qquad (6)$$

resulting from the integration of equation (2) between $y = 0$ and $y = \delta$.

A slag velocity profile of the form

$$u = u_i \left(\frac{y}{\delta}\right)^{\alpha} \qquad (7)$$

is assumed, where the exponent α is treated as an unknown, as in reference 5. This exponent is evaluated only after the expression for the temperature profile is obtained; thus, α serves as a coupling between the energy and momentum equations. From equations (2), (6), and (7), the normal component of the velocity in the slag layer is

$$v = -\frac{m_i}{\rho} \left(\frac{y}{\delta}\right)^{\alpha+1} \qquad (8)$$

where $m_i > 0$ implies slag deposition.

RESULTS AND DISCUSSION

Non-Current-Carrying Slag Layers

The temperature distribution in a non-current-carrying slag layer (i. e., $j = 0$) can now be obtained. Substituting equation (8) into (4) gives

$$\frac{d^2 T}{dy^2} = -\frac{c m_i}{k} \left(\frac{y}{\delta}\right)^{\alpha+1} \frac{dT}{dy} \qquad (9)$$

The solution for the thermal gradient is

$$\frac{dT}{dy} = \frac{q}{k} \exp\left[\frac{-c m_i}{k(\alpha + 2)}\left(\frac{y^{\alpha+2}}{\delta^{\alpha+1}} - \delta\right)\right] \qquad (10)$$

and q is the heat flux from the external flow to the slag layer at the interface. Expanding equation (10) in series form and integrating term by term yields the temperature

4

distribution through the layer as

$$\frac{k}{q}(T - T_w) = \exp\left[\frac{cm_i\delta}{k(\alpha + 2)}\right]\left[y - \frac{cm_i}{k(\alpha + 2)(\alpha + 3)}\frac{y^{\alpha+3}}{\delta^{\alpha+1}} + \ldots\right] \tag{11}$$

For typical values of m_i, c, k, and δ (see table I), we can accurately approximate the temperature distribution by

$$T = T_w + \frac{qy}{k}\exp\left[\frac{cm_i\delta}{k(\alpha + 2)}\right] \tag{12}$$

Slag velocity can now be obtained from equations (3), (5), and (12) as

$$u = \frac{\tau_i}{\mu_i T_i^\beta}\int_0^y\left\{T_w + \frac{q\eta}{k}\exp\left[\frac{cm_i\delta}{k(\alpha + 2)}\right]\right\}^\beta d\eta \tag{13}$$

$$u = D\left(\left\{T_w + \frac{qy}{k}\exp\left[\frac{cm_i\delta}{k(\alpha + 2)}\right]\right\}^{\beta+1} - T_w^{\beta+1}\right) \tag{14}$$

where

$$D \equiv \frac{\tau_i k}{\mu_i T_i^\beta(\beta + 1)q}\exp\left[\frac{-cm_i\delta}{k(\alpha + 2)}\right] \tag{15}$$

Equation (14) can be observed to satisfy the no-slip condition at the wall by setting $y = 0$. Another expression for D incorporating the interface slag velocity can be obtained by evaluating equation (14) at the interface where $y = \delta$, giving

$$D \equiv u_i\left(\left\{T_w + \frac{q\delta}{k}\exp\left[\frac{cm_i\delta}{k(\alpha + 2)}\right]\right\}^{\beta+1} - T_w^{\beta+1}\right)^{-1} \tag{16}$$

Hence,

$$u = u_i \left(\left\{ T_w + \frac{qy}{k} \exp\left[\frac{cm_i \delta}{k(\alpha + 2)} \right] \right\}^{\beta+1} - T_w^{\beta+1} \right) \left(\left\{ T_w + \frac{q\delta}{k} \exp\left[\frac{cm_i \delta}{k(\alpha + 2)} \right] \right\}^{\beta+1} - T_w^{\beta+1} \right)^{-1}$$

(17)

If we evaluate the derivative of u at the slag layer surface from equation (17) and equate this result to that obtained from equation (7), we find with use of equation (12) that

$$\alpha = \frac{(\beta + 1)(T_i - T_w)T_i^\beta}{T_i^{\beta+1} - T_w^{\beta+1}}$$

(18)

The slag layer thickness δ is determined from equation (12) and evaluated at $y = \delta$, expanding the exponential for small arguments, as

$$\delta = \frac{k}{q}(T_i - T_w)\left[1 - \frac{cm_i}{q(\alpha + 2)}(T_i - T_w) \right]$$

(19)

For $m_i = 0$ this result reduces to that obtained in reference 6.

From equations (12) and (14), the interface slag velocity is

$$u_i = \frac{\tau_i k}{\mu_i T_i^\beta q(\beta + 1)} \exp\left[\frac{-cm_i \delta}{k(\alpha + 2)} \right] \left(T_i^{\beta+1} - T_w^{\beta+1} \right)$$

(20)

Substituting values of u_i, δ, and α from equations (18) to (20) into equation (7) will give the velocity profile of non-current-carrying slag layers as a function of slag properties.

The velocity profiles for various values of α are presented in figure 2. One sees that most of the streamwise slag transport occurs near the slag surface when $\alpha \gg 1$. This corresponds to the condition $T_i^{\beta+1} \gg T_w^{\beta+1}$. In this limit, equation (18) reduces to

$$\alpha \simeq (\beta + 1)\frac{T_i - T_w}{T_i} \gg 1$$

(21)

As previously noted, β has a value between 17 and 20. In the limit $T_w \to T_i$, equation (18) reduces to

$$\alpha \simeq 1 + \beta \frac{T_i - T_w}{T_i} \simeq 1 \tag{22}$$

and the velocity profile becomes linear. Figure 3 presents α as a function of T_w for various values of T_i. In figure 4 the analytical result obtained in this report is compared to the more rigorous numerical result of Crawford, et al. (ref. 4). The agreement is excellent. For the case presented in reference 4, the value of T_i gives $\beta \simeq 13$ for equation (5).

Current-Carrying Slag Layers

The temperature variation within a current-carrying slag layer flowing over an infinitely segmented electrode wall is dictated by

$$\frac{d^2T}{dy^2} + \frac{cm_i}{k}\left(\frac{y}{\delta}\right)^{\alpha+1}\frac{dT}{dy} + \frac{j_y^2}{\sigma k} = 0 \tag{23}$$

In the present analysis, an electrical conductivity of the form $\sigma(T) = AT^{\gamma}$ has been assumed (ref. 6). Furthermore, as part of the model, $\sigma(T)$ is replaced by $\sigma(y)$. The relation between T and y needed for the conductivity calculation is provided by equation (12) (i.e., the temperature distribution when $j = 0$). Thus, the conductivity model applies only to cases where the contribution to the temperature distribution by Joule heating is much smaller in magnitude than

$$T_w + \frac{qy}{k}\exp\left[\frac{cm_i\delta}{k(\alpha+2)}\right]$$

In general, this implies j must be less than 10 000 A/m^2 if $T_w \geq 1000$ K and j must be less than 5000 A/m^2 if $T_w < 1000$ K. Using the heat flux at the gas-slag interface as the boundary condition, the first integral of equation (23) is

$$\frac{dT}{dy} = \exp\left[\frac{-cm_i y^{\alpha+2}}{k(\alpha+2)\delta^{\alpha+1}}\right]\left(\frac{q}{k}\exp\left[\frac{cm_i \delta}{k(\alpha+2)}\right]\right.$$

$$\left. + \frac{j^2}{kA}\int_y^\delta \exp\left[\frac{cm_i \eta^{\alpha+2}}{k(\alpha+2)\delta^{\alpha+1}}\right]\left\{T_w + \frac{q\eta}{k}\exp\left[\frac{cm_i \delta}{k(\alpha+2)}\right]\right\}^{-\gamma} d\eta\right) \qquad (24)$$

Expanding those exponential terms that are functions of y for small arguments and integrating the result term by term gives

$$T(y) \simeq T_w + \frac{qy}{k}\exp\left[\frac{cm_i \delta}{k(\alpha+2)}\right] + \frac{j^2\exp\left[\frac{-cm_i \delta}{k(\alpha+2)}\right]}{Aq(1-\gamma)}\left\{T_w + \frac{q\delta}{k}\exp\left[\frac{cm_i \delta}{k(\alpha+2)}\right]\right\}^{1-\gamma} y$$

$$- \frac{j^2 k\exp\left[\frac{-2cm_i \delta}{k(\alpha+2)}\right]}{Aq^2(1-\gamma)(2-\gamma)}\left\{T_w + \frac{qy}{k}\exp\left[\frac{cm_i \delta}{k(\alpha+2)}\right]\right\}^{2-\gamma}$$

$$+ \frac{j^2 k T_w^{2-\gamma}\exp\left[\frac{-2cm_i \delta}{k(\alpha+2)}\right]}{Aq^2(1-\gamma)(2-\gamma)} + \ldots \qquad (25)$$

The remaining terms in this series expression for the temperature variation are at least a factor $cm_i \delta/k(\alpha+2)$ smaller in magnitude. Their contribution is negligible under typical base-loaded conditions. Shown in figure 5 are the temperature distributions at various current densities for two different T_w's and $m_i = 0$. The following two relations have been used to approximate the numbers used for electrical conductivity in reference 4:

$$\sigma = 6.892\times10^{-42}\, T^{13}\ (\text{ohm-m})^{-1}, \quad T > 1341\ \text{K}$$

and

$$\sigma = 1.296\times10^{-10}\, T^3\ (\text{ohm-m})^{-1}, \quad T \le 1341\ \text{K}$$

8

Direct quantitative comparison with the case presented in Crawford, et al. (ref. 4) is not possible since the present electrical conductivity model is not applicable to such a low value of T_w and high value of j.

The slag layer thickness can now be estimated by evaluating equation (25) at $y = \delta$. The exact solution for δ from the ensuing expression is extremely difficult, if not impossible, to obtain analytically. However, since the magnitudes of the terms involving Joule heating effects have already been assumed to be small, the method of successive approximations may be used. As a first approximation, the small Joule heating terms are neglected, resulting in expressions (18) and (19) for α and δ. A better approximation for the slag layer thickness can then be obtained by substituting the first approximation solutions for α and δ into the terms arising from Joule heating effects. The resulting expression is solved for δ. The result can be put in the form

$$\delta \simeq \delta_0(1 + \Psi) \tag{26}$$

where δ_0 is the value of δ when $j = 0$ given by equation (19) and

$$\Psi \equiv -\frac{j^2 k \exp\left(\dfrac{-2cm_i T_i}{\beta q}\right)}{Aq^2(T_i - T_w)(1 - \gamma)(2 - \gamma)} \left[(1 - \gamma)T_i^{2-\gamma} - (2 - \gamma)T_w T_i^{1-\gamma} + T_w^{2-\gamma}\right] \tag{27}$$

The slag velocity from equations (3), (5), and (25) is

$$u(y) = \frac{\tau_i}{\mu_i T_i^\beta} \int_0^y \left(\left(T_w + \frac{q\eta}{k} \exp\left[\frac{cm_i \delta}{k(\alpha + 2)}\right] + \frac{j^2 k \exp\left[\dfrac{-2cm_i \delta}{k(\alpha + 2)}\right]}{Aq^2(1 - \gamma)(2 - \gamma)}\right.\right.$$

$$+ \frac{j^2 \exp\left[\dfrac{-cm_i \delta}{k(\alpha + 2)}\right]}{Aq(1 - \gamma)} \left\{T_w + \frac{q\delta}{k} \exp\left[\frac{cm_i \delta}{k(\alpha + 2)}\right]\right\}^{1-\gamma} \eta$$

$$\left.\left. - \frac{j^2 k \exp\left[\dfrac{-2cm_i \delta}{k(\alpha + 2)}\right]}{Aq^2(1 - \gamma)(2 - \gamma)} \left\{T_w + \frac{q\eta}{k} \exp\left[\frac{cm_i \delta}{k(\alpha + 2)}\right]\right\}^{2-\gamma}\right)^\beta \right) d\eta \tag{28}$$

9

Employing a binomial expansion in the form $(1 + z)^n$, truncated to two terms, gives

$$u(y) = \frac{\tau_i}{\mu_i T_i^{\zeta}} \left\{ \left[\frac{k}{q\lambda(\beta + 1)} + \frac{\beta j^2 k^2 \left(T_w + \frac{q\lambda\delta}{k}\right)^{1-\gamma}}{Aq^3\lambda^3(1 - \gamma)(\beta + 1)} \right] \left[\left(T_w + \frac{q\lambda y}{k}\right)^{\beta+1} - T_w^{\beta+1}\right] \right.$$

$$+ \left[\frac{-j^2 k^2 T_w \left(T_w + \frac{q\lambda\delta}{k}\right)^{1-\gamma}}{Aq^3\lambda^3(1 - \gamma)} + \frac{j^2 k^2 T_w^{2-\gamma}}{Aq^3\lambda^3(1 - \gamma)(2 - \gamma)} \right] \left[\left(T_w + \frac{q\lambda y}{k}\right)^{\beta} - T_w^{\beta}\right]$$

$$\left. - \frac{\beta j^2 k^2}{Aq^3\lambda^3(1 - \gamma)(2 - \gamma)(\beta - \gamma + 2)} \left[\left(T_w + \frac{q\lambda y}{k}\right)^{\beta-\lambda+2} - T_w^{\beta-\lambda+2}\right] \right\} \quad (29)$$

wherein $\lambda \equiv \exp\left[2m_i\delta/k(\alpha + 2)\right]$. The velocity at the interface u_i may be found by evaluating equation (29) at $y = \delta$, noting that at the interface $T_w^{\beta} \ll \left[T_w + (q\lambda\delta/k)\right]^{\beta}$. Thus, the interface velocity may be written as

$$u_i \simeq u_{i0}(1 + \Pi) \quad (30)$$

where u_{i0} is the value of u_i when $j = 0$, given by equation (20), while

$$\Pi \equiv \frac{j^2 k \exp\left[\frac{-2cm_i\delta}{k(\alpha + 2)}\right]}{Aq^2(1 - \gamma)} \left[\frac{\beta(\gamma^2 - \gamma\beta - 4\gamma + \beta + 3)T_i^{1-\gamma} + (\beta + 1)\beta T_w^{2-\gamma+\beta}T_i^{1-\beta}}{(2 - \gamma)(\beta - \gamma + 2)} \right.$$

$$\left. - (\beta + 1)T_w T_i^{-\gamma} + (\beta + 1)T_i^{-1}T_w^{2-\gamma}(2 - \gamma)^{-1} \right] \quad (31)$$

Similarly, comparing the gradient of the velocity at $y = \delta$ evaluated from equation (29) with that evaluated from equation (7) results in

$$\alpha \simeq \alpha_0(1 + \Phi) \quad (32)$$

where α_0 is the value of α when $j = 0$ given by equation (18) and

10

$$\Phi \equiv \frac{j^2 k \, \exp\left(\dfrac{-2cm_i T_i}{\beta q}\right)}{Aq^2(1 - \gamma)}\Bigg[(\beta T_i + T_w)T_i^{-\gamma} - T_w^{2-\gamma}T_i^{-1}(2 - \gamma)^{-1}$$

$$-\frac{\beta(\gamma^2 - \gamma\beta - 5\gamma + 2\beta + 5)T_i^{1-\gamma} + (\beta + 1)\beta T_w^{2-\gamma+\beta}T_i^{-1-\beta}}{(2 - \gamma)(\beta - \gamma + 2)}$$

$$-\frac{(1 - \gamma)T_i^{2-\gamma} - (2 - \gamma)T_w T_i^{1-\gamma} + T_w^{2-\gamma}}{(2 - \gamma)(T_i - T_w)}\Bigg] \tag{33}$$

Typical behavior of Φ and δ as a function of current density, at various T_w's, is shown in figures 6 and 7. As the amount of Ohmic heating is increased, the trend is toward thinner slag layers with more linear velocity profiles.

CONCLUDING REMARKS

Approximate analytical expressions are derived for the velocity and temperature variations in steady-state slag deposits flowing over the magnetohydrodynamic generator walls. Effects of both slag condensation and Joule heating are included in the analysis. In addition to providing trends and physical insight, the derived results enable one to easily determine the internal properties of coal-slag layers once the transport conditions and temperature at the slag-gas interface are known from preliminary calculations and/or experimental measurements. Because of the assumptions in the electrical conductivity model, the results for electric-current-carrying slag layers are not applicable to low-wall-temperature and high-current-density cases.

Lewis Research Center,
National Aeronautics and Space Administration,
Cleveland, Ohio, October 19, 1976,
506-25.

APPENDIX - SYMBOLS

A   a constant

B   magnetic field strength, T

c   specific heat at constant pressure of slag layer, $J/(kg)(K)$

H   heat transfer coefficient, $q(T_\infty - T_i)^{-1}$, $W/(m^2)(K)$

j, j_y normal electric current density, A/m^2

k   thermal conductivity of slag, $W/(m)(K)$

m_i mass transfer rate at slag surface, $kg/(m^2)(sec)$

P   pressure, Pa

P_a gas pressure, Pa

q   heat transfer rate to slag surface from free-stream gas, W/m^2

T   temperature, K

T_i temperature at slag surface, K

T_w wall temperature, K

T_∞ free-stream gas temperature, K

u   velocity parallel to wall, m/sec

u_i velocity of slag at $y = \delta$, m/sec

v   velocity perpendicular to wall, m/sec

x   coordinate parallel to wall

y   coordinate perpendicular to wall

α exponent in velocity profile

β exponent in slag viscosity model

γ exponent in slag electrical conductivity model

δ slag layer thickness, m

μ slag viscosity, $N\text{-}sec/m^2$

μ_i viscosity at slag surface, $N\text{-}sec/m^2$

ρ slag density, kg/m^3

σ electrical conductivity of slag, $(ohm\text{-}m)^{-1}$

τ_i shear stress at slag surface, N/m^2

REFERENCES

1. Shanklin, R. V., et al.: The UTSI Coal Burning MHD Program. Proc. 13th Symposium on Engineering Aspects of Magnetohydrodynamics. Stanford Univ., 1973, Paper No. II. 8.

2. Stickler, D. B.; and DeSaro, R.: Replenishment Analysis and Technology Development. Sixth Int. Conf. on Magnetohydrodynamic Electrical Power Generation. Vol. 2: Open Cycle Components and Materials. CONF-750601-Vol. -2, Int. At. Energy Agency, 1975, pp. 31-49.

3. Crawford, L. W.; et al.: Investigation of Slag Deposits and Seed Absorption in a Direct-Fired MHD Power Generator. Sixth Int. Conf. on Magnetohydrodynamic Electrical Power Generation. Vol. 2: Open Cycle Components and Materials. CONF-750601-Vol. -2, Int. At. Energy Agency, 1975, pp. 51-65.

4. Dicks, J. B.; et al.: Development Program for MHD Direct Coal-Fired Power Generation Test Facility. QPR-1, Univ. Tenn., 1975.

5. McFarland, B. L.; and Harmon, D. B.: Heat Transfer through a Melting Layer with External Gas Flow. Proc. Heat Transfer and Fluid Mech. Inst., R. C. Binder, et al., eds., Stanford Univ. Press, 1961, pp. 208-221.

6. Rosa, R. J.: Design Considerations for Coal Fired MHD Generator Ducts. Fifth Int. Conf. on Magnetohydrodynamic Electrical Power Generation. Vol. 1, Organiation for Economic Co-Operation and Develop. (Munich), 1971, pp. 427-439.

7. Koester, J. K.; et al.: In-Channel Observations on Coal Slag. Proc. 15th Symposium on Engineering Aspects of Magnetohydrodynamics, Univ. Penn., 1976, Paper No. I. 6.

TABLE I. - SOME TYPICAL SLAG PROPERTIES AND PARAMETERS

IN BASE-LOADED GENERATOR DESIGNS

Parameter	Typical value	Reference
Thermal conductivity of slag, k	0.5 to 1.73 W/(m)(K)	3, 6
Slag density, ρ	2.5×10^3 to 3.0×10^3 kg/m^3	2, 3, 6
Specific heat of slag, c	1.382×10^3 N-m/(kg)(K)	2
Slag layer thickness, δ	0.5×10^{-3} to 2.5×10^{-3} m	2, 6
Slag layer Reynolds number	10^{-1}	2
Heat transfer coefficient, $q/(T_\infty - T_i)$	1.43×10^3 W/(m^2)(K)	3, 4
Rate of slag deposit, m_i	3.0×10^{-3} to 2.8×10^{-2} kg/(m^2)(sec)	6
Shear stress at slag surface, τ_i	$P_a\times10^{-3}$ pascals	6
Interface velocity, u_i	~0.4 m/sec	2, 4
Gas-slag interface temperature, T_i	1550 to 2000 K	2, 6
Wall temperature, T_w	500 to 2000 K	2, 4, 6
Free-stream gas temperature, T_∞	2700 to 2800 K	2, 4, 7
Free-stream gas pressure, P_a	0.5×10^5 to 4×10^5 pascals	6
Magnetic induction, B	4 to 5 T	-----
Pressure gradient, dp/dx	$-P_a\times10^{-1}$ pascals	6
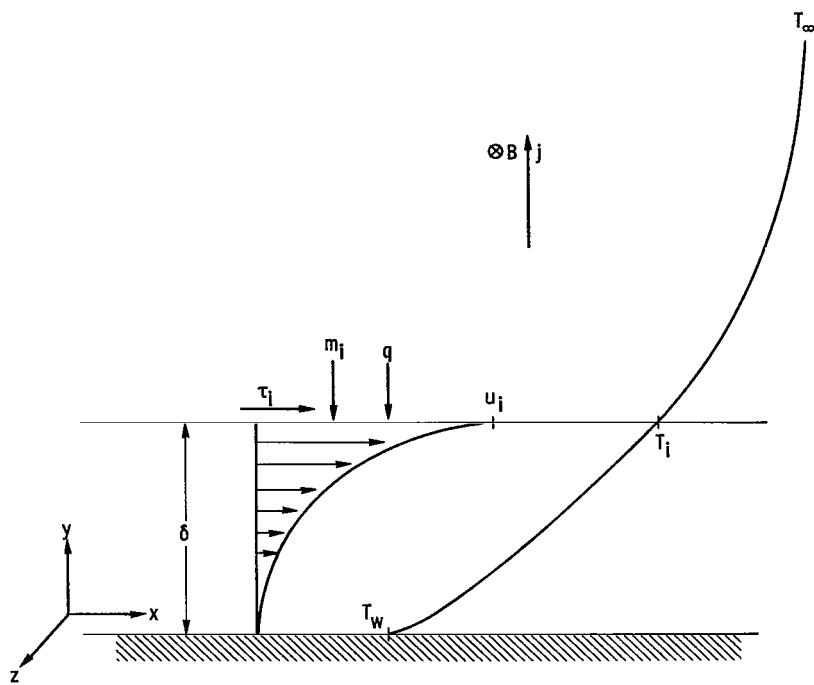
Figure 1. – Schematic of slag layer.
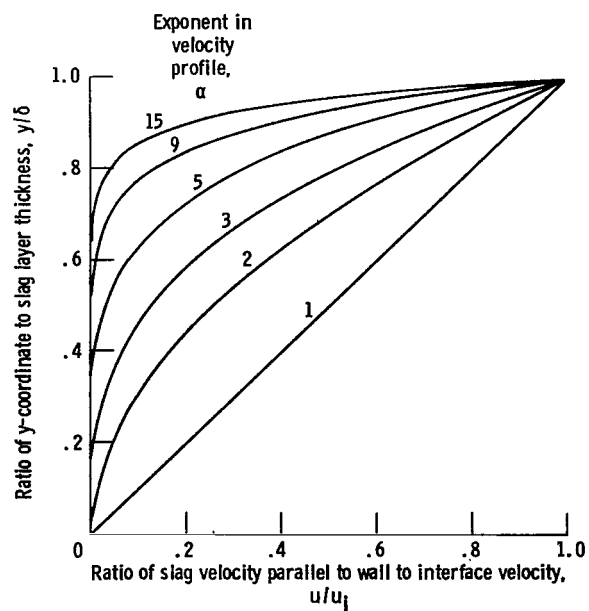
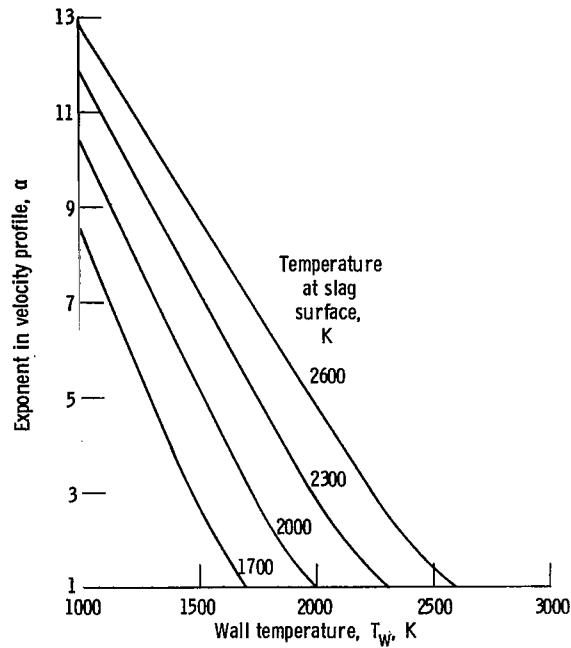Figure 2. – Slag layer velocity profiles, equation (7), for representative values of α.

Figure 3. - Velocity profile exponent as a function of wall temperature at various slag surface temperatures. Exponent in slag viscosity model, β, 20; normal electric current density, j, 0.
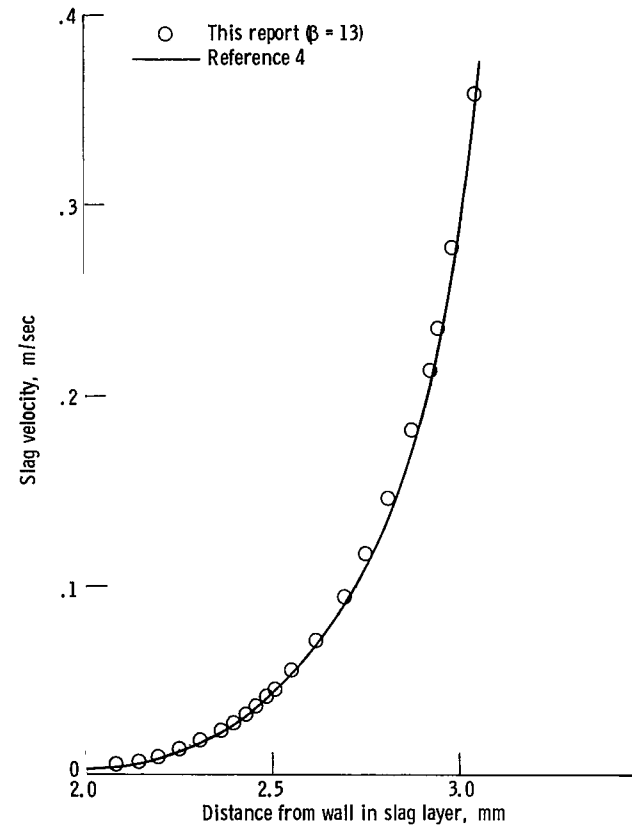

Figure 4. - Comparison with results of Crawford, et al. (ref. 4). Thermal conductivity of slag, k, 1.73 W/(m)(K); interface velocity, 0.36 m/sec; normal electric current density, j, 0; free-stream gas temperature, T_∞, 2700 K; wall temperature, T_w, 500 K; temperature at slag surface, T_i, 2075 K; heat transfer coefficient, H, 1430 W/(m^2)(K); mass transfer rate at slag surface, m_i, 0.
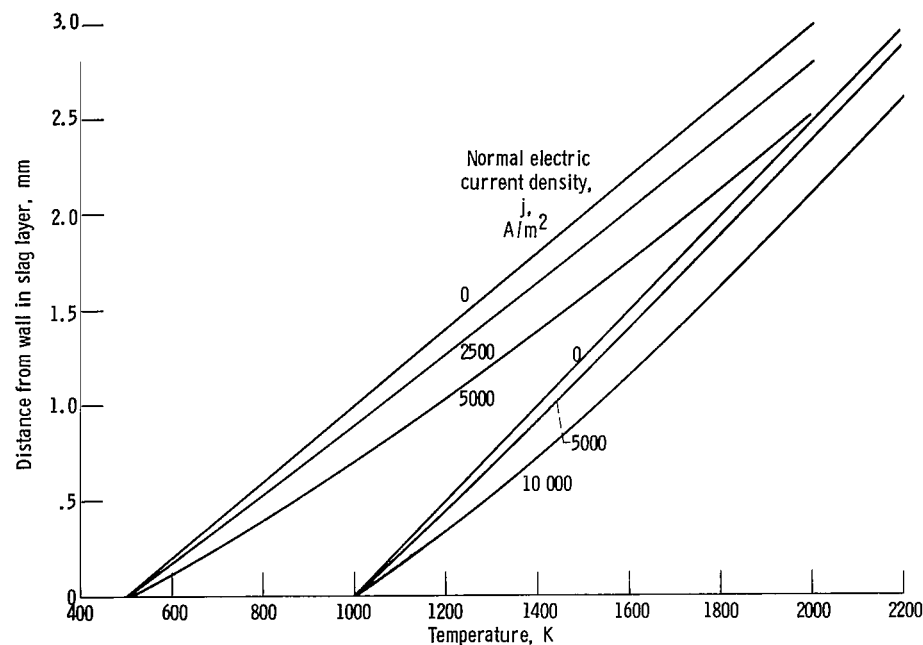
Figure 5. - Temperature distribution in slag layer for various current densities at wall temperatures of 500 and 1000 K. Thermal conductivity of slag, k, 1.73 W/(m)(K); free-stream gas temperature, T_∞, 2700 K; heat transfer coefficient, H, 1430 W/(m²)(K); mass transfer rate at slag surface, m_i, 0; electrical conductivity of slag, σ, 6.892147×10^{-42} T^{13} at T > 1341 K and 1.296×10^{10} T^3 at T ≤ 1341 K.
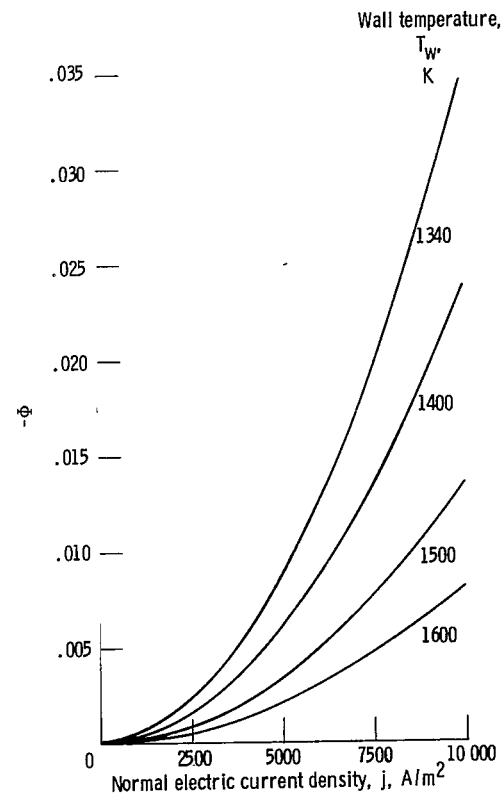

Figure 6. - Typical behavior of Φ as function of current density. Exponent in velocity profile, $\alpha = \alpha_0(1 + \Phi)$; thermal conductivity of slag, k, 1.73 W/(m)(K); free-stream gas temperature, T_∞, 2700 K; heat transfer coefficient, H, 1430 W/(m²)(K); mass transfer rate at slag surface, m_i, 0; exponent in slag viscosity model, β, 20.
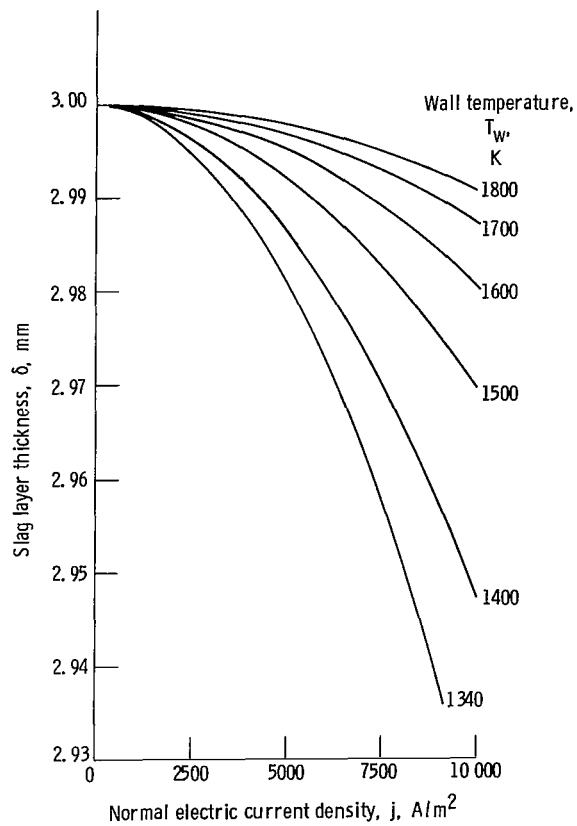
Figure 7. - Typical behavior of slag layer thickness as function of normal electric current density. Thermal conductivity of slag, k, 1.73 W/(m)(K); free-stream gas temperature, T_∞, 2700 K; heat transfer coefficient, H, 1430 W/(m^2)(K); mass transfer rate at slag surface, m_i, 0; exponent in slag viscosity model, β, 20; slag layer thickness at j = 0, δ_0, 3 mm.

"The aeronautical and space activities of the United States shall be conducted so as to contribute . . . to the expansion of human knowledge of phenomena in the atmosphere and space. The Administration shall provide for the widest practicable and appropriate dissemination of information concerning its activities and the results thereof."
—NATIONAL AERONAUTICS AND SPACE ACT OF 1958

NASA SCIENTIFIC AND TECHNICAL PUBLICATIONS

TECHNICAL REPORTS: Scientific and technical information considered important, complete, and a lasting contribution to existing knowledge.

TECHNICAL NOTES: Information less broad in scope but nevertheless of importance as a contribution to existing knowledge.

TECHNICAL MEMORANDUMS: Information receiving limited distribution because of preliminary data, security classification, or other reasons. Also includes conference proceedings with either limited or unlimited distribution.

CONTRACTOR REPORTS: Scientific and technical information generated under a NASA contract or grant and considered an important contribution to existing knowledge.

TECHNICAL TRANSLATIONS: Information published in a foreign language considered to merit NASA distribution in English.

SPECIAL PUBLICATIONS: Information derived from or of value to NASA activities. Publications include final reports of major projects, monographs, data compilations, handbooks, sourcebooks, and special bibliographies.

TECHNOLOGY UTILIZATION PUBLICATIONS: Information on technology used by NASA that may be of particular interest in commercial and other non-aerospace applications. Publications include Tech Briefs, Technology Utilization Reports and Technology Surveys.

Details on the availability of these publications may be obtained from:

SCIENTIFIC AND TECHNICAL INFORMATION OFFICE

NATIONAL AERONAUTICS AND SPACE ADMINISTRATION
Washington, D.C. 20546